



1st International Conference on the Material Point Method, MPM 2017

Modelling strains of soft soils

Hans Teunissen^{a,*}, Cor Zwanenburg^a

^a*Deltares, Boussinesqweg 1, Delft 2629HV, The Netherlands*

Abstract

Deformations in soft soil are generally large due to the low stiffness. This behaviour requires a large deformation continuum approach. Here the focus will be on the strength of soft soils, especially peat. Peat is modelled with an elastic model with isotropic undrained shear strength. This study shows that elasticity and plasticity become entangled for soft materials. It is shown that classical solutions of plasticity theory do not apply for these materials, because the elastic component of the strains does not become negligible. And the small strain plasticity theory underestimates the strength of soft materials. The first part describes the simulations of a strip footing problem on soft soil. The second part describes a plate bearing test on peat in a large triaxial test apparatus and the numerical simulation of this experiment. The same simple model has been used to analyse this test. The simulation captures the essential features of the test i.e. the load curve and deformation pattern.

© 2016 The Authors. Published by Elsevier Ltd.

Peer-review under responsibility of the organizing committee of the 1 st International Conference on the Material Point Method.

Keywords: elasticity; plasticity; finite-element modelling; laboratory tests; failure.

1. Introduction

The top layers of soil in the western part of the Netherlands consist of very soft soils as peat and organic clay. Nevertheless this part of the country is densely populated, implying many building activities in and on these soft soil layers. The mechanical behaviour of these soft soils is topic of this study.

In modelling much focus has been put on the constitutive modelling of clay and peat. For clay this results in for instance anisotropic Camclay types of models [13]. For peat there is yet no clear model that captures all phenomenological aspects (such as anisotropy, fibre contribution among others). In this study we will not focus on

* Corresponding author.

E-mail address: hans.teunissen@deltares.nl

the constitutive model but on the interaction between strength and stiffness. For soft materials large deformations are considered to be essential. The literature on constitutive models formulated consistently in a large deformation context with failure is limited.

This exploratory study investigates the importance of a large deformation formulation for soft materials. A simple constitutive model based on uniform undrained strength will be used. The simulations have been performed with Plaxis 2D 2012.01. It will be shown in a large deformation context that even for this simple model stiffness and strength both influences the limit load. It will be shown that softer materials can be stronger than stiff materials even if the undrained strength is identical. This behaviour is important because it suggests that when strength properties from the laboratory experiments are applied for problems in a large deformation context may give increase in strength. A practical example is for instance the stability assessment of dikes on soft soil. In the current practice large deformations are neglected, which might lead to an underestimation of dike stability.

Nomenclature

ρ	density
B	total plate width
p'	effective isotropic stress
q	deviatoric stress
q_{max}	maximum deviatoric stress
E	Young's modulus
$E_{50,u}$	Young's modulus at 50% failure load for undrained loading
c	cohesion
F_t	failure load

2. Continuum approach and constitutive model

There are numerous different numerical formulations available to describe large strain deformations, such as Updated Lagrange, Total Lagrange [1], Arbitrary Eulerian Lagrange [8], Coupled Eulerian Lagrange [10], Material Point Method [11], and Smoothed Particle Hydrodynamics [6,7] among others. These formulations have been developed to increase applicability of the large strain deformations formulation for a wider range of problems. In this study an Updated Lagrange scheme is used [5] as implemented in Plaxis.

The applied model is an elastic perfect plastic material model. The elastic stiffness is stated in the Young's modulus E and in Poisson's ratio ν . The objective rate of the Cauchy stresses and the symmetric part of the strain rate tensor follow the linear elastic relationship. This elastic law is not adequate for large deformations, a closed cycle of load application and load removal yield energy dissipation in some cases [4]. This may affect the results of the simulations because it will be shown that the elastic contribution to the strains is not negligible to the plastic ones. The plasticity is described by the Tresca yield function and plastic potential.

3. Simulations

3.1. Rigid footing on undrained soil

Problem definition

The rigid footing problem is a simplified analysis of an experiment on peat on a test site in The Netherlands. The soil parameters are based on laboratory and field probe tests [14]. The shear strength was in the order of 7.5 kN/m^2 and is modelled with the standard Mohr-Coulomb model. The undrained Young's modulus was determined from 14 isotropic consolidated triaxial tests, see Figure 1. It is estimated that for the field conditions with $p' \approx 10 \text{ kN/m}^2$ that $E_{50,u} = 500 \text{ kN/m}^2$ is a realistic value for the Young's modulus together with a Poisson's ratio of 0.495. The simulation assumes weightless soil.

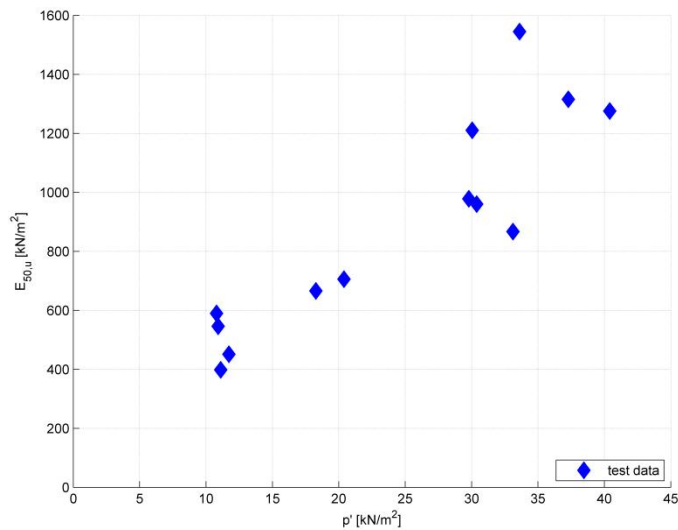


Fig. 1. Test data for undrained Young's moduli, $E_{50,u}$.

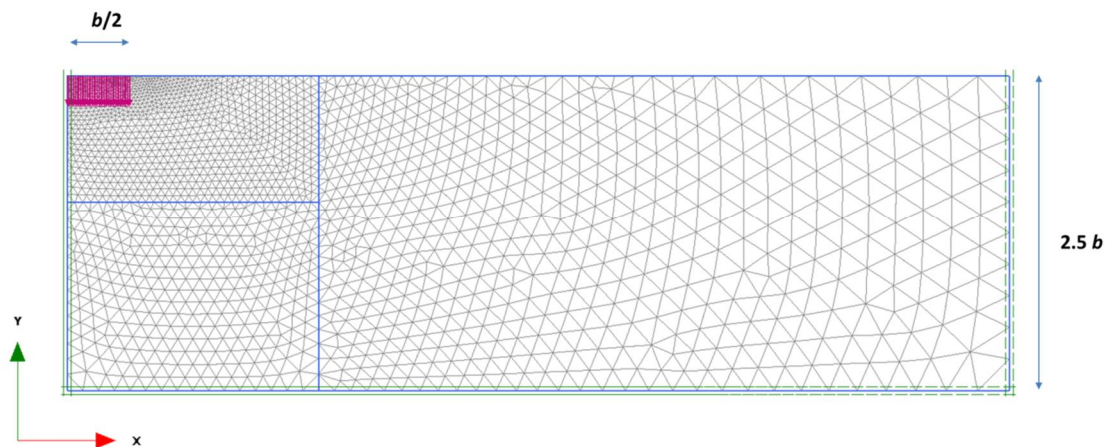


Fig. 2. Mesh used in the analysis.

The mesh of the footing problem contains 3743 6-noded elements and is presented in Figure 2. Half of the symmetrical problem has been modelled with a strip width of $B/2=1$ m. The single soil layer has a thickness of $2.5B$ in the simulation and width of $7.5B$. The boundary at the bottom is smooth. The rigid strip footing is rough.

Comparison with small strains

A comparison is made between the large strain approach (Updated Lagrange) and the small strain approach. In order to make a successful comparison it is required that the deformations in the large strain approach remain small. This is obtained by using a very high Young's modulus, here $E=500000$ kN/m^2 . The stiffness in the small strain approach is of no relevance, here $E=500$ kN/m^2 . The theoretical limit load of a rough footing for small strain conditions is $F_t = (2 + \pi) * c * B/2 \approx 38.562$ kN/m [3]. The loads in the load-displacement curves, Figure 3,

are divided by this theoretical limit load. The displacements of the footing are multiplied with $E/(B c)$ for a dimensionless presentation.

The large and small strain results are almost identical when the material is stiff in the large strain approach. The absolute displacements differ considerably in this comparison but the failure mechanisms and the stresses are similar. The numerical solutions overestimate the theoretical failure load slightly.

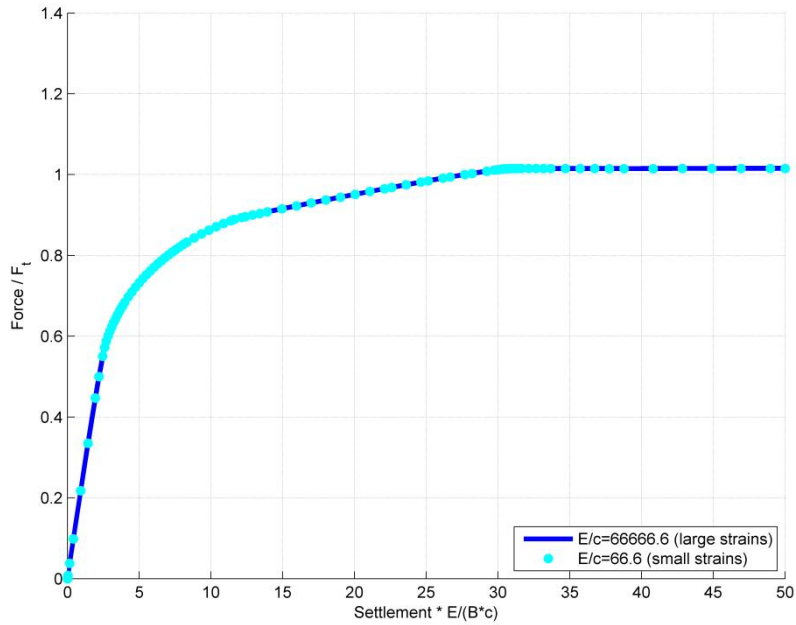


Fig. 3. Comparison of the load-displacement for a stiff material in large deformations with a soft material in small deformations.

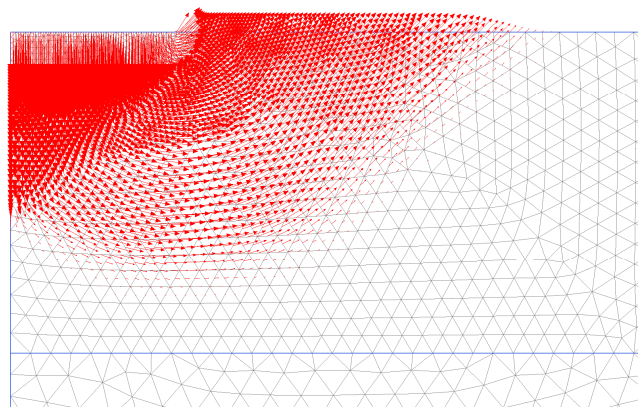


Fig. 4. Detail of the resulting incremental displacements at failure of the stiff material (large strain formulation).

The resulting failure mechanism in Figure 4 shows a Prandtl type of mechanism. The large strain simulation results in the classical small strain solution for high stiffness of the soil. For lower stiffness of the soil there is an increase of load in a large strain simulation, because the geometrical change becomes important. The small strain simulation, although yielding the classical solution, gives unrealistic results for soft soils. In Figure 4 is the footing $0.75 \cdot B$ below the surface while the deformation mechanism is maximum $0.8 \cdot B$ below the surface. The vertical strains below the footing are 30% this precludes a small strain approach.

Large deformations in soft soils

The load-displacement curves for stiffnesses ranging from 500 kN/m^2 to 500000 kN/m^2 are shown in Figure 5. The bearing capacity increases when the material becomes softer and shows no stationary value.

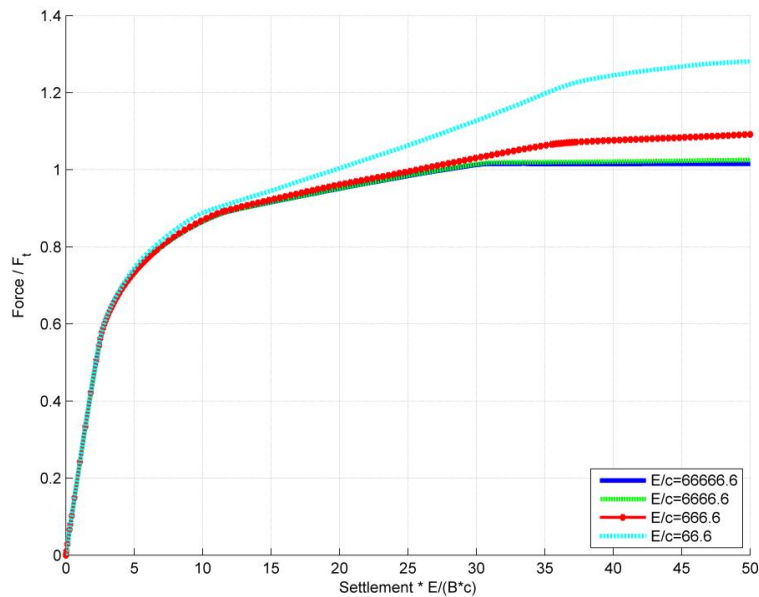


Fig. 5. Comparison of the load-displacement curves for materials in large deformations approach.

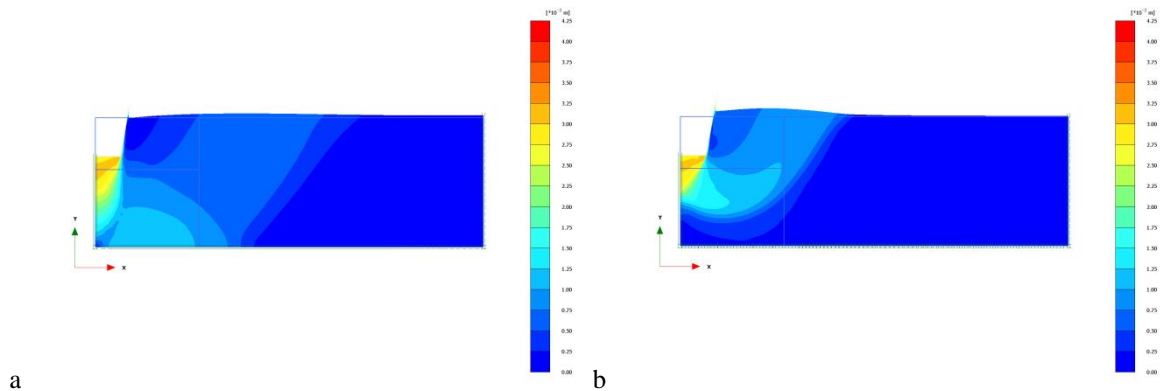


Fig. 6. The resulting incremental displacements at failure at large strains. (a) Results for a smooth bottom. (b) Results for a rough bottom.

The failure mechanism (see Figure 6a) for the soft material is a punching through and not a Prandtl mechanism. This result is similar to the findings of Nazem *et al.* [9]. Next to the footing a peak in the incremental displacements is found that does not seem fully regular. This is caused either by the displacement singularity at the end of the plate or is due to the Updated Lagrange implementation.

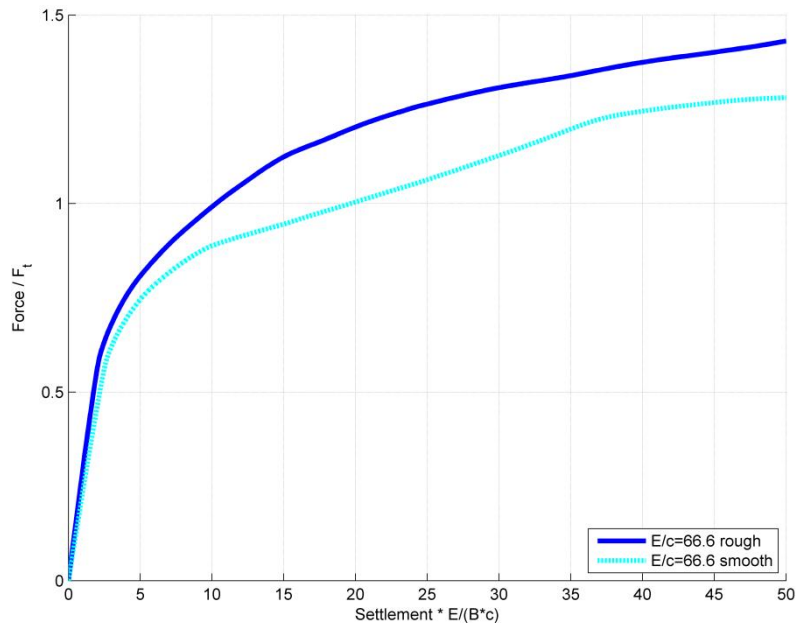


Fig. 7. Comparison of the load-displacement for soft material in large deformations approach with a rough or smooth lower boundary.

The bearing capacity of the footing is influenced by the boundaries when the displacements increase. Figure 6 shows the failure mechanisms for a soft material with a smooth and rough bottom boundary. Figure 7 shows the difference in the load-curves for a soft material. A rough condition at the bottom gives an increase the bearing capacity. The deformation mechanism is smaller and clearly influenced by the lower boundary. In case of the smooth boundary there is a point where the soil yields from the footing to the smooth boundary at the bottom, the load-curve becomes less steep for further displacements.

Figure 5 shows that the bearing capacity of soft soils in this geometry is essentially higher in comparison to classical limit analysis. The computational results show that there is no unique failure load, because after yielding there is a redistribution of stress depending on the boundary conditions. For a soft material a significant elastic strain component of deformations remains at failure and this becomes only clear in a large deformation approach. The bearing capacity in a large deformation continuum approach is not only influenced by the strength properties and dilatancy [12], but also by the stiffness properties, weight and boundary conditions.

3.2. Plate bearing test in a large triaxial set-up

The effect of the stiffness peat on the strength is demonstrated by plate bearing experiment. Figure 8 shows an impression of the plate bearing tests on peat conducted in laboratory conditions [2]. This paper uses these tests to study the influence of a large strain formulation in analysing test data by finite element calculations.

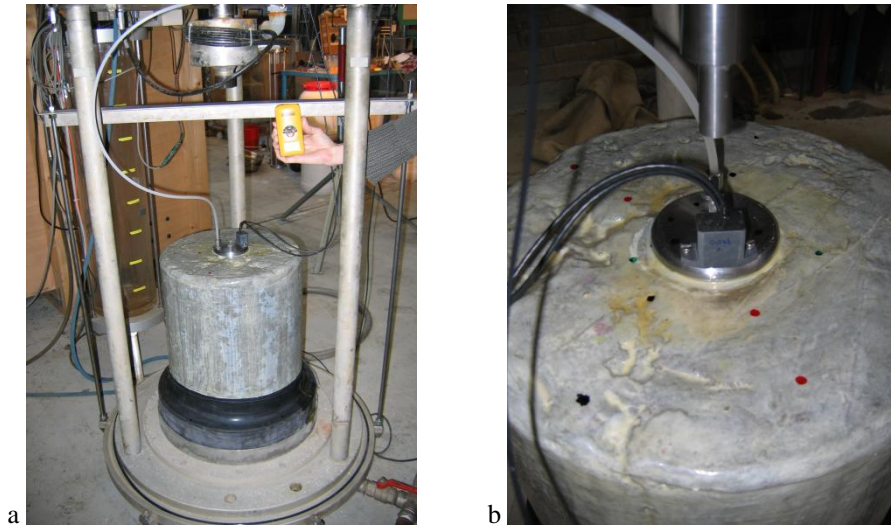


Fig. 8. Impression of test set up for plate bearing test. (a) Peat test 7a. (b) Peat test 7b.

Two plate bearing tests on peat samples were conducted together with one large scale triaxial test. The plate bearing tests were conducted on samples with a diameter of 0.38 m and a height of 0.40 m. The sample is placed in a porous stone. On top of this sample a plate with a diameter of 0.09 m was placed. The centre of the plate coincided with the centre of the sample. Next the sample was covered by a membrane. After placing a cell and filling the cell, the sample is consolidated at a cell pressure of 50 kN/ m². Finally, the plate is pushed down without allowing for drainage.



Fig. 9. Impression of plate bearing test results. (a) Peat test 7a. (b) Peat test 7b.

Figure 9 gives an impression of the results. No sliding planes were observed. The plate was pushed down leaving a clear cut hole behind it. The diameter of this hole was smaller than the diameter of the plate which can be explained by some horizontal displacement. No significant heave of the original surface nor outward displacement at

the outer radius was observed. After finishing the test the sample was cut open. Below the plate a cone of strongly compressed peat was found.

Table 1. Basic properties of the tested peat, derived from large scale triaxial compression test.

Parameter	value
water content, w	540 %
density, ρ	1030 [kg/m ³]
Young's modulus, $E_{50, u}$	1344 [kN/m ²]
Poisson's ratio	0.0
maximum deviator stress, q_{max}	52.66 [kN/m ²]
parameter	value

For parameter assessment one large scale triaxial compression test and a series of conventional triaxial tests were conducted (see Table 1).

The plate bearing test results are simulated with the linear elastic perfect plastic model in an undrained simulation with a constitutive model for the effective stresses and high bulk modulus for the pore water. The parameters follow from Table 1. In the simulation the increase of isotropic stress as applied in the experiment is not been modelled. This has no effect because the constitutive model is independent of the isotropic stress level.

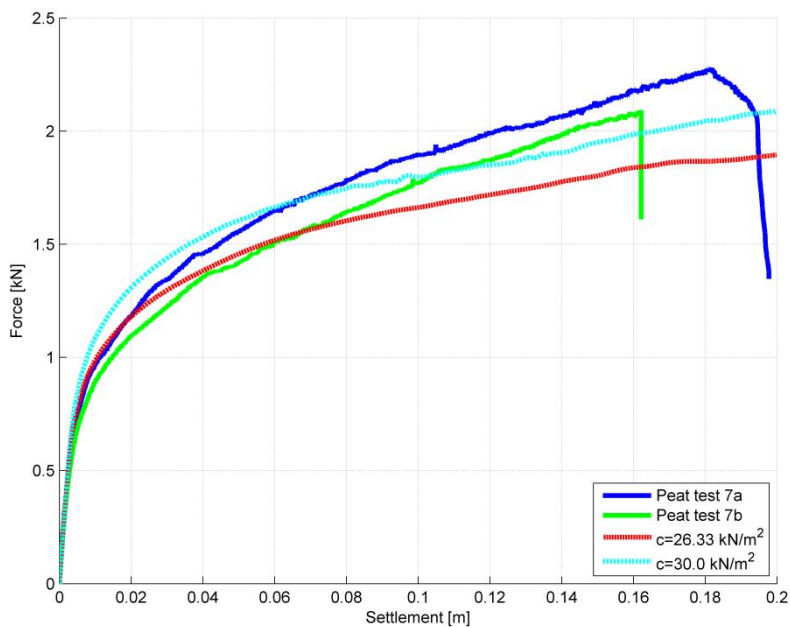


Fig. 10. Load-displacement curves of plate tests on peat with the numerical simulations of the experiments.

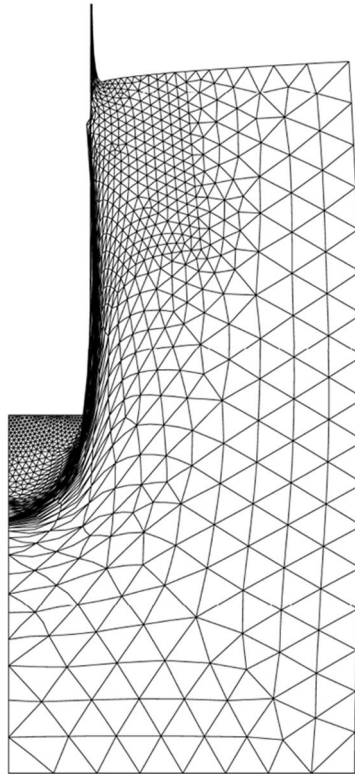


Fig. 11. Deformed mesh (true scale) at the end of the plate test in the large triaxial apparatus.

The results of the simulation (see Figures 10 and 11) match well the experiments on peat. In the experiments it was found that plunger was pushed in to the sample without significant rise of the surface. This is also found in the numerical simulations apart from the irregularity just next to the plate in simulation. Unclear is how much this irregular behaviour influences the result. The load curves do agree with the experimental results. The load increase in the numerical simulations is lower compared to the experiments for higher displacements of the plunger.

The small strain approach with the same material characterization would lead to a shallow deformation mechanism with heave of the surface and a limit load of 1.05 kN/m^2 . This is way off the experimental results.

4. Conclusions

In a large strain formulation of soft soils the bearing capacity results is not only influenced by the strength properties but also by the stiffness properties, weight and the boundary conditions.

This study shows that it is possible to simulate the plate bearing tests on peat in the large triaxial apparatus quite accurately with a simple constitutive model but with a large strain approach.

The mechanical description of soft soils requires a large strain continuum formulation. Without this approach the (geo-)mechanical behaviour is not well understood. The classical expressions for the bearing capacity are not applicable because the elasticity cannot be neglected; the stiffness of these materials is so low that it is essential to incorporate the change of the geometry.

Reconsideration of the definition for failure load is necessary in relation with the boundary conditions, since for soft soil conditions a monotonic increase in shear strength is found for increasing shear strain. This implies that a more specific approach is needed then as what would follow from the classical limit analysis.

The numerical simulations require a more robust large strain approach than the Updated Lagrange formulation, because the shape of the elements is not controlled in such a formulation. Moreover it is necessary to develop and to

test constitutive models for soft soils in a large deformation continuum approach so that parameters and numerical model agree.

Acknowledgements

We would like to thank the Dutch Ministry of Public Works, Rijkswaterstaat, for supporting this research.

References

- [1] K.J. Bathe, Finite element procedures, Upper Saddle River, New Jersey: Prentice Hall, 1996.
- [2] A. van Duinen, “SBW Werkelijke sterkte van dijken, WS01 Analyse veld- en laboratoriumonderzoek”, Deltares-Report 1001463-022-GEO-0001 (in Dutch), 2010.
- [3] R. Hill, The mathematical theory of plasticity, Oxford: Oxford University press, 1950.
- [4] J. Huetink, On the simulation of thermo-mechanical forming processes, PhD thesis TU Twente, 1986.
- [5] H. van Langen, Numerical analysis of soil-structure interaction, PhD thesis TU Delft, 1991.
- [6] L.D. Libersky, A.G. Petschek, Smooth Particle Hydrodynamics with Strength of Materials, Advances in the Free Lagrange Method, Lecture Notes in Physics 395 (1990), 248–257.
- [7] L.D. Libersky, A.G. Petschek, A.G. Carney, Hipp T.C., Allahdadi J.R., High F.A., Strain Lagrangian hydrodynamics: a three-dimensional SPH code for dynamic material response, J. Comput. Phys. 109 (1993), 67–75.
- [8] W.K. Liu, T. Belytschko, H. Chang., An arbitrary Lagrangian-Eulerian FE-method for path-dependent materials, Comp. Meth. App. Mech. Eng. 58 (1986), 227-245.
- [9] M. Nazem, D. Sheng, J.P. Carter, Stress integration and mesh refinement for large deformation in geomechanics, Int. J. Numer. Meth. Engng 65 (2006), 1002-1027.
- [10] W. Noh CEL: a time-dependent, two-space-dimensional, coupled Eulerian–Lagrangian code, Methods in Computational Physics 3, 1964, 117–179.
- [11] D. Sulsky, Z. Chen, H.L. Schreyer, A particle method for history-dependent materials, Computer Methods in Applied Mechanics and Engineering 118 (1994), 179-196.
- [12] J.A.M. Teunissen, On double shearing in friction, Int. J. Numer. Anal. Meth. Geomech. 31 (2007), 23–51.
- [13] S.J. Wheeler, A. Nääätänen, M. Karstunen, M. Lojander, An isotropic elastoplastic model for soft clays, Can. Geotech. J. 40 (2003), 403-418.
- [14] C. Zwanenburg, M.A. Van, Full Scale field tests for strength parameter assessment, Proceedings of the 18th International Conference on Soil Mechanics and Geotechnical Engineering, Paris 2013.